https://doi.org/10.5194/esd-2024-34
Preprint. Discussion started: 30 October 2024

Earth System Dynamics Discussions

Future changes in spatiotemporal precipitation patterns of the East Asian summer monsoon and associated uncertainty factors

Yeon-Hee Kim[1], Seung-Ki Min[1,2]

[1]Division of Environmental Science and Engineering, Pohang University of Science and Technology, Pohang, 37673, South Korea
[2]Institute for Convergence Research and Education in Advanced Technology, Yonsei University, Incheon, 21983, South Korea

Correspondence to: Seung-Ki Min (skmin@postech.ac.kr)

Abstract. East Asia has been identified as a key area at risk of precipitation increases resulting from global warming. East Asian summer monsoon has distinct spatiotemporal characteristics and the simulation characteristics of global climate models therefore needs to be evaluated closely to obtain a reliable projection of future precipitation patterns and associated extreme events. Using metrics for the spatiotemporal variability of monsoon precipitation over East Asia, this study evaluated the performance of Coupled Model Intercomparison Project Phase 6 (CMIP6) models and analyzed future projections and uncertainty factors. Spatiotemporal precipitation patterns were simulated reasonably well by CMIP6 models but with weaker rainfall amplitudes. CMIP6 models simulated more intense precipitation than the predecessor CMIP5 ones and captured observations better. In future projections, an overall precipitation increase occurs during both the northward migration of the rain band and during peak monsoon time over East Asia and the three subregions, with stronger changes under higher emission scenarios. This increase was mainly ascribed to a thermodynamic response due to increased moisture availability. Internal climate variability and model uncertainty dominated future precipitation uncertainties. Dynamic terms explained a large portion of model uncertainty due to circulation changes, and thermodynamic terms were significantly related to scenario uncertainty.

1 Introduction

The East Asian summer monsoon is an important large-scale circulation system occurring across countries such as China, Korea, and Japan. The monsoonal rain band moves northward over East Asia from May to July, and its precipitation exhibits complex spatiotemporal patterns influenced by internal climatic variability (e.g., influences of the El Niño–Southern Oscillation) and topography (e.g., the Tibetan Plateau). The Intergovernmental Panel on Climate Change (IPCC) identified East Asia as one of the key risk regions where statistically significant climate change causing heavy precipitation can be expected as a result of a 1.5 ℃ or, even greater consequence, a 2 ℃ global warming scenario (Hoegh-Guldberg et al., 2018). Such change would deliver a huge socioeconomic impact on the densely populated region. Consequently, to establish a reliable projection of future shifts in precipitation over East Asia, the performance of global climate models (GCMs) must be evaluated closely, and further climatic projections alongside uncertainty assessments are essential.

https://doi.org/10.5194/esd-2024-34
Preprint. Discussion started: 30 October 2024

A new generation of GCMs has been released for the Coupled Model Intercomparison Project Phase 6 (CMIP6) experiments (Eyring et al., 2016). The CMIP6 ensembles comprise a complex range of models, from GCMs to Earth System Models, with improved physical parameterization and finer spatial resolution than earlier models (Eyring et al., 2016; Marotzke et al., 2017). Recent studies have confirmed that the CMIP6 models provide an advanced simulation of monsoon precipitation compared to CMIP5 ones, especially in terms of precipitation intensity (Chen et al., 2021; Jiang et al., 2020; Kim et al., 2020; Wang et al., 2021; Xin et al., 2020). CMIP6 models can simulate a more realistic climatological pattern of the East Asian summer monsoon, better capturing the northward movement of the monsoonal rain band due to finer horizontal resolutions (Chen et al., 2021; Jiang et al., 2020) and smaller model biases in sea surface temperature (SST) over the Northwestern Pacific Ocean (Xin et al., 2020).

The Asian summer monsoon domain is one of the region most vulnerable to global warming (IPCC, 2013). An increased mean and extreme precipitation have been consistently projected for this region under Representative Concentration Pathway (RCP) scenarios (IPCC, 2013; Kitoh et al., 2013; Endo and Kitoh 2014; Freychet et al., 2015; Li et al., 2015; Lee et al., 2017; Park and Min 2019). Recent studies based on the CMIP6 ensemble have also predicted that precipitation will increase over East Asian monsoon regions by about 8–14% under four Shared Socioeconomic Pathway (SSP) scenarios (SSP1-2.6, SSP2-4.5, SSP3-7.0, and SSP5-8.5) and by 5.6% ℃-1 across a long-term period (2081–2100) under the SSP5-8.5 scenario (Chen et al., 2020; Ha et al., 2020; Moon and Ha 2020); they also suggested that the thermodynamic effects resulting from increased moisture levels may play a dominant role in elevating precipitation levels. These results are consistent with those produced via CMIP5 modeling (Endo and Kitoh 2014; Lee et al., 2017).

Although model simulation performance has improved, uncertainties remain regarding future precipitation projections. These uncertainties tend to increase at a smaller regional scale and with stronger future radiative forcing (Chen et al., 2020). Sources of uncertainty in climate projections consist of three factors: anthropogenic forcing agents, parametric and structural model uncertainties related to the response of the climate model to specified forcing agents, and natural internal variability intrinsic to the climate system (Hawkins and Sutton 2009, 2011). In global mean precipitation projections using the CMIP6 ensemble, model uncertainty plays the dominant role of these three factors, with internal variability and scenario uncertainty contributing to the total uncertainty in the near term (2021–2040) and long term (2081–2100), respectively (Lehner et al., 2020). For the global land monsoon area, model uncertainty dominates the projection uncertainty (~90%), whereas the contribution of internal variability decreases and that of scenario uncertainty increases over time via the CMIP5 ensemble (Zhou et al., 2020).

Previous CMIP6 analyses of monsoon precipitation have focused on summer mean precipitation within the monsoon region. Understanding the changes in spatiotemporal precipitation patterns along the monsoon band is important. However, comprehensive research is lacking on model performance, future projections, and uncertainty in this regard. The objectives of the present study are as follows: 1) to compare the performance of CMIP6 and CMIP5 models in predicting spatiotemporal precipitation patterns in East Asia; 2) to investigate projections of spatiotemporal precipitation patterns and sources of model uncertainty using CMIP6 models under four SSP scenarios; and 3) to examine the uncertainty factors associated with physical mechanisms of change in spatiotemporal precipitation patterns

https://doi.org/10.5194/esd-2024-34
Preprint. Discussion started: 30 October 2024

Earth System Dynamics Discussions
Open Access
EGU

2 Data and methods

2.1 Data

We used daily precipitation data from 25 CMIP6 (Table S1; Eyring et al., 2016) and 22 CMIP5 models (Table S2; Taylor et al., 2012). These models were selected based on their availability of data regarding daily precipitation. To match future forcing levels, we selected the SSP1-2.6, SSP2-4.5, and SSP5-8.5 scenarios from CMIP6 (O'Neil et al., 2016) and the RCP2.5, RCP4.5, and RCP 8.5 scenarios from CMIP5 (Taylor et al., 2012). For model evaluation, historical simulations were used for CMIP6, and historical simulations for CMIP5 were extended to 2014 by combining them with the RCP 4.5 simulations. The evaluation and reference period was selected as 1995–2014. We used the first realization for each model and each scenario, and we present projections for three specific future periods, namely, the near term (NT; 2021–2040), mid term (MT; 2041–2060), and long term (LT; 2081–2100).

The CMIP5 and CMIP6 historical simulations were evaluated against pentad precipitation data retrieved from the Global Precipitation Climatology Project (GPCP; Adler et al., 2018) and Climate Prediction Center Merged Analysis of Precipitation (CMAP; Xie and Arkin 1997) datasets. All observations and model precipitation data were re-gridded into a 2.5° × 2.5° resolution prior to further analysis

2.2 Indices of spatiotemporal precipitation patterns

To analyze spatiotemporal rainfall patterns, three East Asian subregions (Fig. S1) were defined as China (20–45°N, 110–120°E), Korea (20–45°N, 120–130°E), and Japan (20–45°N, 130–142°E), following Kusunoki and Arakawa (2015). The whole East Asian domain encompasses the domain of 15–50°N, 100–150°E. To define precipitation indices that can explain spatiotemporal patterns, the rainy season was classified into two indices according to the movement of the monsoonal rain band. Figure 1 shows the latitude–time cross-section of precipitation climatology that depicts the zonal averages for East Asia and the three subregions, as derived from GPCP, CMAP, CMIP6 Multi-Model Ensemble (MME), and CMIP5 MME data. In general, from mid-May to June, the monsoon band moved northward from lower latitudes (around 20–25°N), reaching the mid-latitudes (around 30–35°N) by July (Fig. 1).

We defined our two precipitation indices by averaging the precipitation at (1) the time of northward movement of the monsoon band and (2) the peak of the monsoon band. An index of northward migration (hereafter referred to as "northward migration") was defined as the average precipitation during June between 20°N and 35°N in the entire East Asian region, 20°N and 32.5°N in China, and 25°N and 35°N in both Korea and Japan (red boxes in Fig. 1). The peak time index (hereafter referred to as "peak time") was defined as the average precipitation during July between 30°N and 40°N in East Asia, 27.5°N and 37.5°N in China, and 32.5°N and 42.5°N in both Korea and Japan (blue boxes in Fig. 1).

https://doi.org/10.5194/esd-2024-34
Preprint. Discussion started: 30 October 2024

Earth System Dynamics Discussions

95 To examine the meridional movement of the monsoon band under different climate change scenarios, we defined the monsoon band location. The fourth-order centered difference was used to calculate the meridional precipitation gradient, and the latitude with maximum precipitation (*d* precipitation / *d* latitude = 0) was determined using linear interpolation.

2.3 Uncertainty partitioning

100 To examine the source of uncertainty in future precipitation projection, we employed the method developed by Hawkins and Sutton (2009, 2011) where total uncertainty (*T*) consists of the internal variability (*I*), model uncertainty (*M*), and scenario uncertainty (*S*). Each term can be estimated as a variance across a given time (*t*) as follows:

$$T(t) = I(t) + M(t) + S(t) \quad (1)$$

This equation assumes that sources of uncertainty are independent. The fractional uncertainties (%) were furthermore 105 calculated as $I(t)/T(t)$, $M(t)/T(t)$, and $S(t)/T(t)$.

The response to radiative forcing was estimated as a fourth-order polynomial fit to the precipitation change (%) of each model over the 1995–2100 period. The reference precipitation was determined using 1995–2014 means. Before regression fitting, the time series of precipitation change (1995–2100) was smoothed using the decadal running mean to reduce noise. Internal variability (*I*) was then calculated as the multi-model mean of the variance of the residuals from the fourth-order polynomial 110 fits for a given model; internal variability does not change over time. Secondly, the model uncertainty (*M*) for each scenario was estimated from the variance of fitted values in different model simulations; model uncertainty components were considered to represent the multi-scenario mean. Lastly, scenario uncertainty (*S*) was calculated as the variance in the multi-model mean obtained for the three scenarios. For further details, refer to Hawkins and Sutton (2009, 2011).

2.4 Moisture budget analysis

115 To analyze the contribution of thermodynamic and dynamic mechanisms in future precipitation changes, we conducted a moisture budget analysis based on the linearized equation following previous studies (Seager and Naik 2012; Gao et al., 2012; Endo and Kitoh 2014; Li et al., 2015; Lee et al., 2017, 2018):

$$\delta P = \delta E + \delta TH + \delta DY + \delta NL + \mathrm{res} \quad (2)$$

$$\delta TH = -\frac{1}{\rho_w g}\int_0^{p_s} \nabla \cdot (\bar{u}_{\mathrm{REF}}[\delta \bar{q}])\mathrm{d}p \quad (3)$$

120 $$\delta DY = -\frac{1}{\rho_w g}\int_0^{p_s} \nabla \cdot ([\delta \bar{u}]\bar{q}_{\mathrm{REF}})\mathrm{d}p \quad (4)$$

$$\delta NL = -\frac{1}{\rho_w g}\int_0^{p_s} \nabla \cdot (\delta \bar{u}\delta \bar{q})\mathrm{d}p \quad (5)$$

$$\delta(\cdot) = (\cdot)\mathrm{LT} - (\cdot)\mathrm{CLIM} \quad (6)$$

where P is precipitation; E is surface evaporation; TH, DY, and NL are the thermodynamic, dynamic, and nonlinear terms, respectively; u is the horizontal wind vector; q is the specific humidity; p is the pressure; ρ_w is the water density; g is the

https://doi.org/10.5194/esd-2024-34
Preprint. Discussion started: 30 October 2024


Earth System Dynamics Discussions Open Access EGU

gravitational acceleration; and p_s is the surface pressure. CLIM and LT indicate the climatology (1995–2014) and long-term periods (2081–2100), respectively. The unit of all terms is mm day-1. Overbars indicate climatological monthly means.

To analyze future precipitation changes, we considered E, TH, DY, and NL, which were calculated using monthly mean values. Before the analysis, the evaporation, surface pressure, zonal wind, meridional wind, and specific humidity data were re-gridded into a 2.5° × 2.5° resolution. Vertical integration of the TH, DY, and NL terms was conducted at six pressure levels: 1000, 850, 700, 500, 250, and 100 hPa.

3 Results

3.1 Spatiotemporal precipitation patterns

Before analyzing future rainfall projections, we evaluated the climatology of spatiotemporal precipitation patterns. The CMIP6 and CMIP5 model ensembles generally reproduced the observed climatology patterns of the seasonal precipitation cycle in East Asia and its three subregions (Fig. 1). However, the two CMIPs showed weaker amplitudes than the two observations, particularly at the peak time. However, The CMIP6 models simulated more intense precipitation than the CMIP5 models (Fig. S2).

In East Asian domain, the observed monsoon band moved northward from 20°N during June and reached 35°N in July. Both CMIP6 and CMIP5 faithfully reproduced this precipitation pattern during both the northward migration and the peak time of monsoon band. The CMIP6 ensemble captured the observed climatology more closely than the CMIP5 MME (Fig. S2). However, dry biases remained during the peak time. The location of the monsoon band was simulated well by both CMIPs.

In the China subregion, northward movement of the rain band occurred between 20°N and 32.5°N in June and approached 35°N in July (i.e., the "Mei-yu" frontal systems). The seasonal cycle of precipitation over China simulated by both the CMIP6 and CMIP5 MMEs was similar to that of the observed pattern, although the models underestimated the extent of northward migration of the monsoon band. The CMIP6 MME exhibited a better predictive performance of precipitation than CMIP5, but the dry biases remained in the monsoon band of the CMIP6 ensemble (Fig. S2). Additionally, both CMIPs located the rain band further north than the observations.

In Korea and Japan, the monsoon band moved northward from 25°N to 30°N in June and approached 40°N in July, as deduced from the GPCP and CMAP datasets (i.e., the frontal system termed "Changma" in Korea and "Baiu" in Japan). Both the CMIP5 and CMIP6 MMEs underestimated precipitation during the rainy season. Critically, neither model simulated a precipitation higher than that actually observed during the peak time in Korea, and only one model (MIROC6) simulated more precipitation than what was observed during the northward migration of the monsoon band. Moreover, the CMIP6-modeled rainband reached a similar latitude to that of the observed band during the peak time in Korea. The precipitation dry bias of the CMIP6 MME was also reduced during the northward migration of the rain band in Japan (Fig. S2).

The CMIP6 and CMIP5 MME future projections of zonal mean precipitation over the long term are displayed in Figure 2. Precipitation is predicted to increase along the monsoon band in all future scenarios. Stronger increases were recorded in higher

https://doi.org/10.5194/esd-2024-34
Preprint. Discussion started: 30 October 2024


Earth System Dynamics Discussions Open Access EGU

emission scenarios (SSP5-8.5 and RCP8.5). CMIP6 models generally simulated a stronger intensification in precipitation than CMIP5 models. Despite the increase in precipitation along the monsoon band, the location of the monsoon band remained unchanged over East Asia and the three subregions.

Overall, both CMIP5 and CMIP6 reproduced the observed seasonal cycle well, with dry biases in East Asia and the three subregions. Of the two, the CMIP6 model generally improved the precipitation simulation of the monsoon band, particularly in terms of its northward migration. The projected enhanced precipitation is consistent with the findings of previous studies (Chen et al., 2021; Jiang et al., 2020; Xin et al., 2020). Therein, the improved performance of the CMIP6 model was ascribed to its use of a higher spatial resolution (Chen et al., 2021; Jiang et al., 2020) and its expression of smaller SST biases over the Northwestern Pacific Ocean (Xin et al., 2020).

To illustrate the details of projected changes in precipitation over East Asia and its three subregions, Figure 3 presents the northward migration and peak time of the monsoon band for our selected three future periods. The CMIP6 models projected, using three SSP and RCP scenarios, that precipitation will increase during both the northward migration and peak time of the monsoon band over East Asia and its three subregions. Generally, the change in precipitation rate was dependent on different emission scenarios and the length of the future period; precipitation was projected to increase appreciably under higher emission scenarios and over long-term periods. The uncertainty range was also the widest in the higher-emission scenario and over the long-term period.

Under SSP1-2.6, SSP2-4.5, and SSP5-8.5, precipitation was projected to increase over the long-term in our East Asian domain by 9.8% (4.5–15.0% for the ±1 standard deviation range), 10.4% (4.6–16.1%), and 16.4% (8.2–24.6%), respectively, during the northward migration of the monsoon band, and by 9.4% (0.8–18.0%), 9.7% (2.9–16.5%), and 12.9% (3.5–22.4%), respectively, during the peak time (Fig. 3). For both the northward migration and peak time of the monsoon, more than two-thirds of the models agreed on the positive sign of the precipitation change, implying that most models could project robust changes over long-term periods. Overall, the precipitation projections of the CMIP5 and CMIP6 models were similar. Precipitation change during the northward monsoon band migration tended to be larger than that of the peak time in future scenarios of climate change projected by both CMIPs, except for the RCP2.6 scenario. However, in CMIP6, inter-model variability for peak time precipitation was larger than that projected for the period of northward migration of the monsoon band.

When analyzing projection results for the subregions, precipitation was enhanced over China from 11% to 20% during the northward migration of the monsoon band and from 9% to 13% during the peak time in the long-term period of three SSP scenarios (Fig. 3). In the case of CMIP6 models for Korea, this precipitation increase was robust for the long-term period, at 8–17% for the northward migration and 12–16% for the peak time. In Japan, precipitation was predicted to increase from 12% to 18% during the northward migration of the rain band and from 9% to 13% for the peak time over the long term. Notably, over Korea, precipitation increases were projected for both the northward migration and peak time of the monsoon, whereas for China and Japan, the precipitation showed a stronger intensification during the northward migration of the rain band. In CMIP6, the uncertainty range associated with peak time was larger than that for the northward migration of the monsoon band

https://doi.org/10.5194/esd-2024-34
Preprint. Discussion started: 30 October 2024

for all three subregions. In contrast, the CMIP5 models displayed a larger uncertainty range for precipitation change during the northward migration of the rain band. Overall, CMIP6 models simulated more intense precipitation changes than CMIP5 models under the same radiative forcing scenario, except for Japan when considering a higher emission scenario.

3.2 Uncertainty factors

To examine how the uncertainty inherent to precipitation projections differ between models, we investigated the changes in total uncertainty as portioned among its three components as previously identified: *I*, *M*, and *S*. Figure 4 shows the total fraction of variance for the two CMIPs as obtained when analyzing three different future time periods. In the near-term period analysis, *I* and *M* were the dominant contributors to projection uncertainty. Depending on the region, the contribution of *I* decreased slightly, while that of *M* increased slightly for the mid-term period analysis. In the long-term period analysis, the contribution of *M* to total uncertainty was dominant, that of *I* decreased, and that of *S* increased slightly (to less than 10% on average). The contributions of all three of these components to projection uncertainty were similar for projections encompassing either East Asia or the three subregions individually.

M was the dominant contributor to CMIP6 projections of precipitation change during both the northward migration of the rain band and peak time throughout the 21st century, which is consistent with analyses of global mean precipitation and monsoon land precipitation projections (Hawkins and Sutton 2011; Lehner et al., 2020; Zhou et al., 2020). However, in our study, the contribution of *I* was crucial in the near-term period analysis, whereas that of *S* remained small. The corresponding results when using CMIP5 showed a similar pattern.

3.3 Moisture budget analysis

To determine the mechanism of precipitation change in future projections, we conducted a moisture budget analysis, which investigated how thermodynamic and dynamic mechanisms influence such projections of the spatiotemporal pattern of East Asian precipitation. Figure 5 illustrates the change in precipitation and moisture budget terms over a long-term period analysis using CMIP5 and CMIP6 for three climate change scenarios over East Asia and its three subregions. The precipitation increases during the northward migration of the rain band and peak monsoon time chiefly corresponded with an increase in *TH* and a general decrease in *NL*. Increased precipitation was associated with either a decrease or increase in *DY*, depending on the region. We could, therefore, conclude that *TH* plays a more dominant role in the occurrence of intense precipitation (due to increased moisture availability) than DY and NL. These results are consistent with those of previous studies (Chen et al., 2020; Endo and Kitoh 2014; Lee et al., 2017, 2018).

Figure 6 shows the relationship between the MME precipitation change and *TH*, which combines three climate change scenarios from the two CMIPs over a long-term analysis period. When considering the northward shift of the rain band, the relationship between the MME precipitation change and *TH* was statistically significant at the 10% level (based on a *t*-test)

https://doi.org/10.5194/esd-2024-34
Preprint. Discussion started: 30 October 2024

across the MMEs, including all six scenarios over all regions, except for China and Korea during the peak monsoon time. This again implies that *TH* explains a large part of *S* when conducting long-term period projections.

To examine the contribution of *DY* to inter-model uncertainty, we analyzed the relationship between precipitation change and *DY* across models for the long-term period projections of precipitation changes (Fig. 7). Precipitation change was significantly correlated with *DY* using three scenarios in the two CMIPs for all regions, except for the SSP2-4.5 and SSP5-8.5 scenarios over East Asia and the RCP8.5 scenario over Korea during peak time. This indicates that *DY* contributed to model uncertainty in long-term period projections, that is, the spread of the CMIP6 and CMIP5 models in future precipitation projections was mainly caused by uncertainty regarding circulation changes.

4 Summary and conclusion

To quantify the spatiotemporal variability of precipitation patterns in East Asia and three subregions, we defined two indices based on (1) the northward migration of the monsoon band and (2) the peak time of the monsoon. Using this metric, we evaluated and compared projections in precipitation change between CMIP6 and CMIP5 models of various climatic scenarios. We also analyzed sources of projection uncertainty under three SSP scenarios for three future periods (near-term, mid-term, and long-term) and determined the relative contributions of TH and DY to uncertainty based on a moisture budget analysis.

The CMIP6 models reproduced the observed climatology patterns of spatiotemporal variability in precipitation well, and the overall performance of the CMIP6 MME was improved compared to that of the CMIP5 MME. However, dry bias remained in the CMIP6 MME. The models projected that precipitation would exhibit an overall increase during both the northward migration of the rain band and during peak monsoon time over East Asia and the three subregions. This projected increase in precipitation was greater for the period of northward migration than for the peak time over all regions, except for Korea. However, inter-model variability was greater during the peak time than during the northward migration of the rain band. Intense precipitation was predicted over the long term and was associated with thermodynamic responses due to increased moisture availability. M and I were the main contributors to the total uncertainty of precipitation projections. For long-term projections, S accounted for approximately 10% of the total variance. The inter-model variability in precipitation change was mainly caused by differences in DY resulting from circulation changes across the models while TH was significantly associated with S.

Our results for the CMIP6 model performance and future projections were consistent with those of previous global and Asian monsoon precipitation studies based on different metrics (Chen et al., 2020, 2021; Moon and Ha 2020; Xin et al., 2020). In terms of spatiotemporal variations in precipitation, the simulation performance of CMIP6 models was superior to that of CMIP5 and CMIP3 (Kusunoki and Arakawa 2015). This may be attributable to the higher spatial resolution and improved model physics of CMIP6 (cf. Eyring et al., 2019; Paik et al., 2020). To confirm the spatial resolution effect, future research can utilize the multi-tiered HighResMIP subproject of CMIP6, which enables the systematic investigation of the resolution impact for the past and future climate (Haarsma et al., 2016). Some studies reported that increased spatial resolution did not

https://doi.org/10.5194/esd-2024-34
Preprint. Discussion started: 30 October 2024

Earth System Dynamics
Discussions
Open Access
EGU

change model skill metrics appreciably, depending on regions (e.g., Xin et al., 2021; Wehenr et al., 2021), which indicates the importance of assessing physical processes associated with the spatiotemporal precipitation patterns.

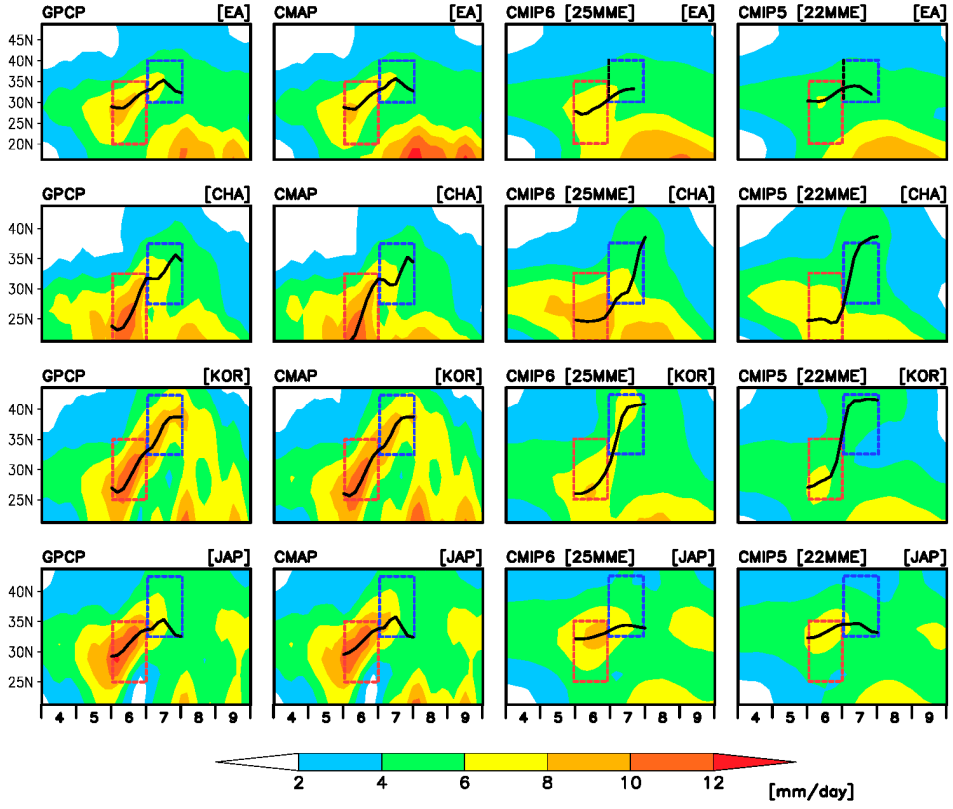

255

Figure 1. Time–latitude cross sections of pentad precipitation rates (mm/day) from 1995 to 2014 over East Asia (EA; 100–150°E), China (CHA; 110–120°E), Korea (KOR; 120–130°E), and Japan (JAP; 130–142°E) from the Global Precipitation Climatology Project (GPCP), Climate Prediction Center Merged Analysis of Precipitation (CMAP), Coupled Model Intercomparison Project Phase 6 (CMIP6) Multi-Model Ensemble (MME), and CMIP5 MME. Red and blue boxes represent the northward migration and
260 **peak time of monsoon rain bands, respectively. Black lines follow the latitude with the precipitation maximum (dPR/dlat = 0).**

https://doi.org/10.5194/esd-2024-34
Preprint. Discussion started: 30 October 2024

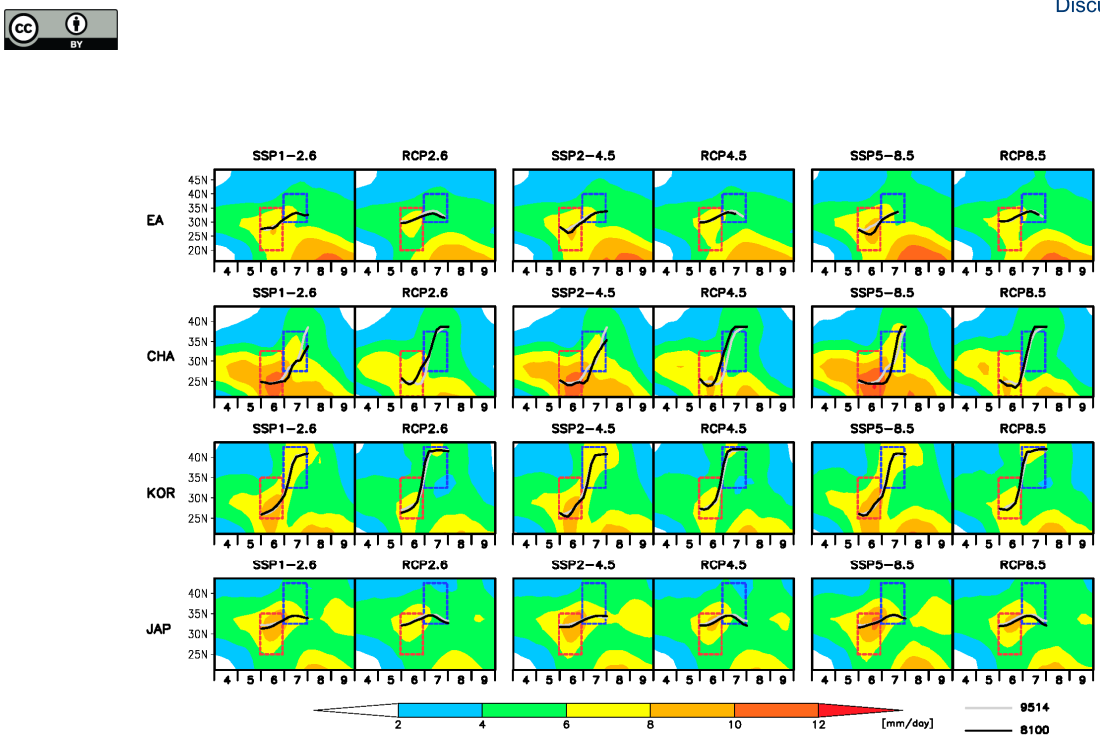

Figure 2. Time–latitude cross sections of pentad precipitation (mm/day) over East Asia (EA), China (CHA), Korea (KOR), and Japan (JAP) in a long-term period (2081–2100) from six future scenarios : Shared Socioeconomic Pathway (SSP)1-2.6, Representative Concentration Pathway (RCP)2.6, SSP2-4.5, RCP4.5, SSP5-8.5, and RCP8.5. Red and blue boxes represent the northward migration and peak time of monsoon rain bands, respectively. The gray and black lines follow latitudes with the precipitation maximum in 1995–2014 and in 2081–2100, respectively.

https://doi.org/10.5194/esd-2024-34
Preprint. Discussion started: 30 October 2024

Earth System Dynamics
Discussions
Open Access
EGU

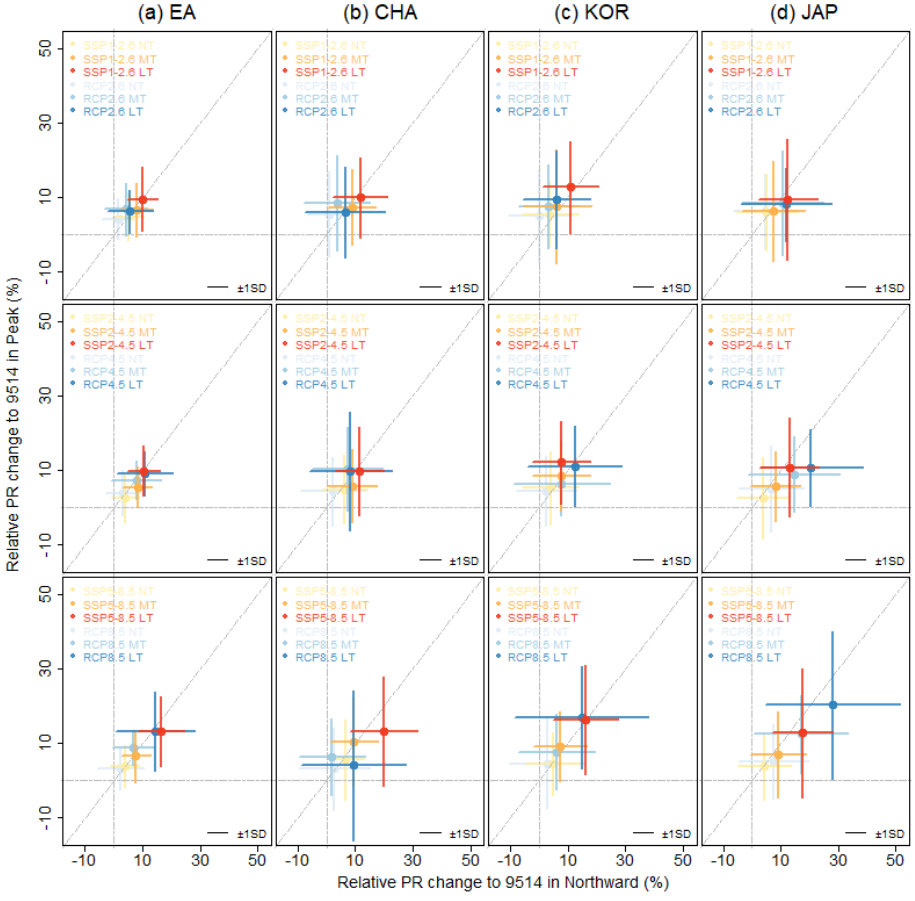

Figure 3. Scatter plot of changes in precipitation (PR) during the northward migration (x-axis) and peak time (y-axis) of the monsoon band over (a) East Asia (EA), (b) China (CHA), (c) Korea (KOR), and (d) Japan (JAP) for near-term (NT; 2021–2040), mid-term (MT; 2041–2060), and long-term (LT; 2081–2100)) from six future scenarios: Shared Socioeconomic Pathway (SSP)1-2.6 and Representative Concentration Pathway (RCP) 2.6 (1st row), SSP2-4.5 and RCP4.5 (2nd row), and SSP5-8.5 and RCP8.5 (3rd row). Projections are based on the climatological data during 1995–2014. Error bars indicate ±1 standard deviation (SD) for values calculated via the Coupled Model Intercomparison Project Phase 6 and Phase 5 models.

https://doi.org/10.5194/esd-2024-34
Preprint. Discussion started: 30 October 2024

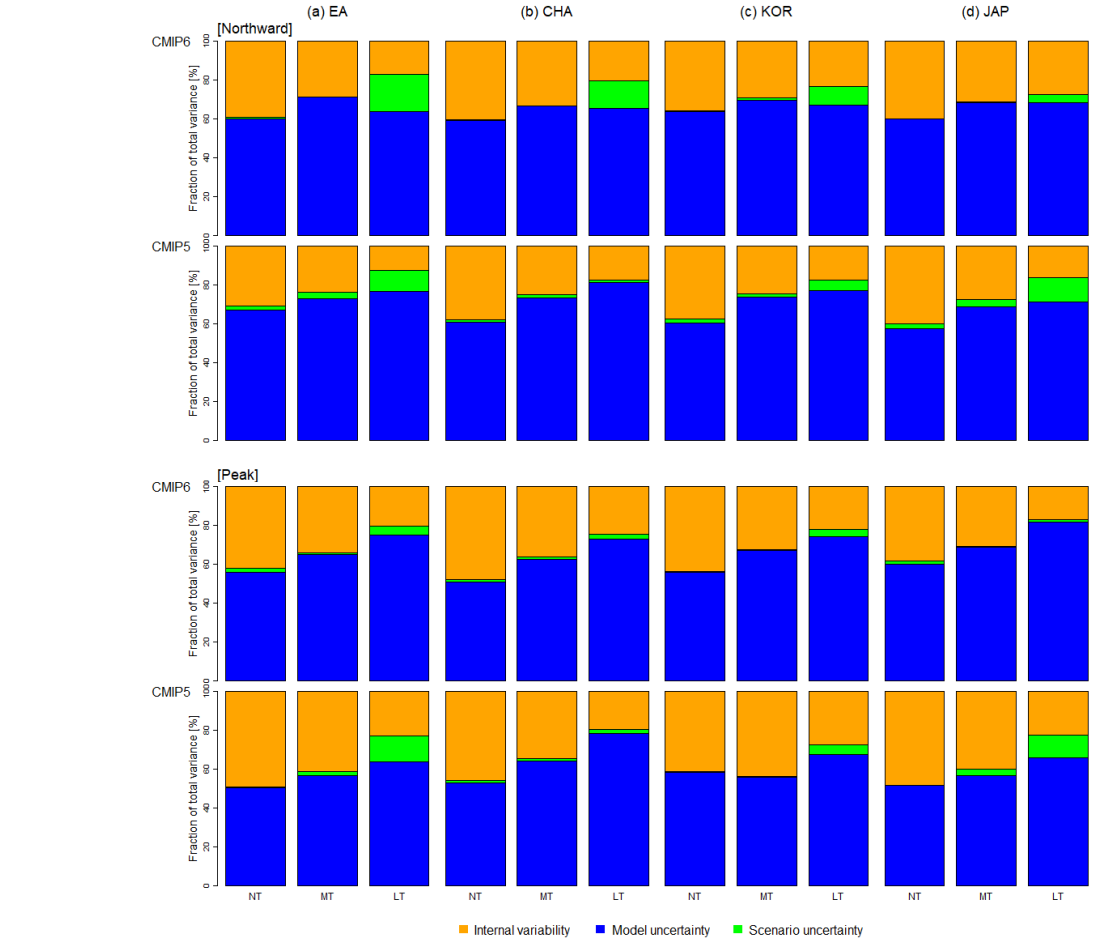

Figure 4. Relative contributions (%) of internal variability (orange), model uncertainty (blue), and scenario uncertainty (green) to variance in total predictive uncertainty for near-term (NT), mid-term (MT), and long-term (LT) models of precipitation change over (a) East Asia (EA), (b) China (CHA), (c) Korea, and (d) Japan (JAP) for the northward migration (upper two panels) and the peak time (bottom two panels) of the monsoon band. The top panel in each of these two sets illustrates results obtained via CMIP6, while the bottom panel contains results obtained with CMIP5.

https://doi.org/10.5194/esd-2024-34
Preprint. Discussion started: 30 October 2024

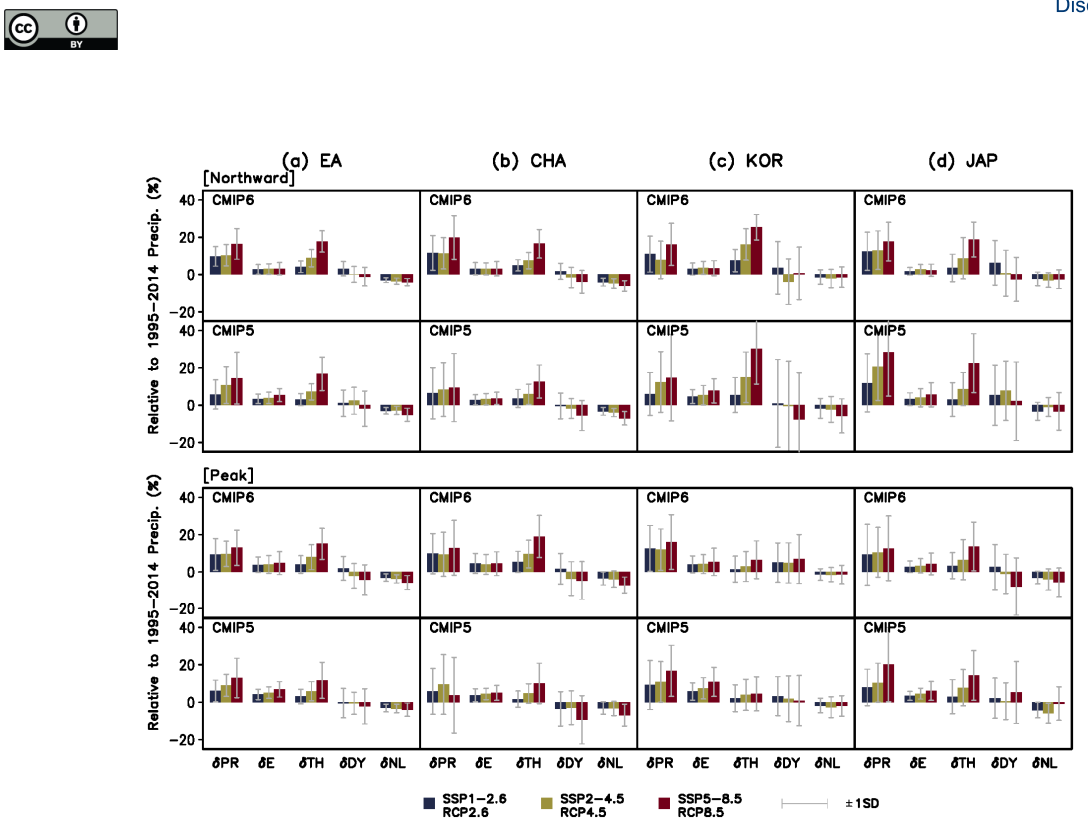

Figure 5. Change in moisture budget terms—precipitation (PR), evaporation (E), thermodynamic (TH), dynamic (DY), and nonlinear (NL)—for long-term (2081–2100) analyses over (a) East Asia (EA), (b) China (CHA), (c) Korea (KOR), and (d) Japan (JAP), relative to the climatology during 1995–2014 from six future scenarios: Shared Socioeconomic Pathway (SSP)1-2.6 and Representative Concentration Pathway (RCP)2.6 (blue bars), SSP2-4.5 and RCP4.5 (green bars), and SSP5-8.5 and RCP8.5 (dark red bars). Gray error bars indicate the ±1 standard deviation (SD) range of the models.

https://doi.org/10.5194/esd-2024-34
Preprint. Discussion started: 30 October 2024

Earth System Dynamics
Discussions
Open Access
EGU

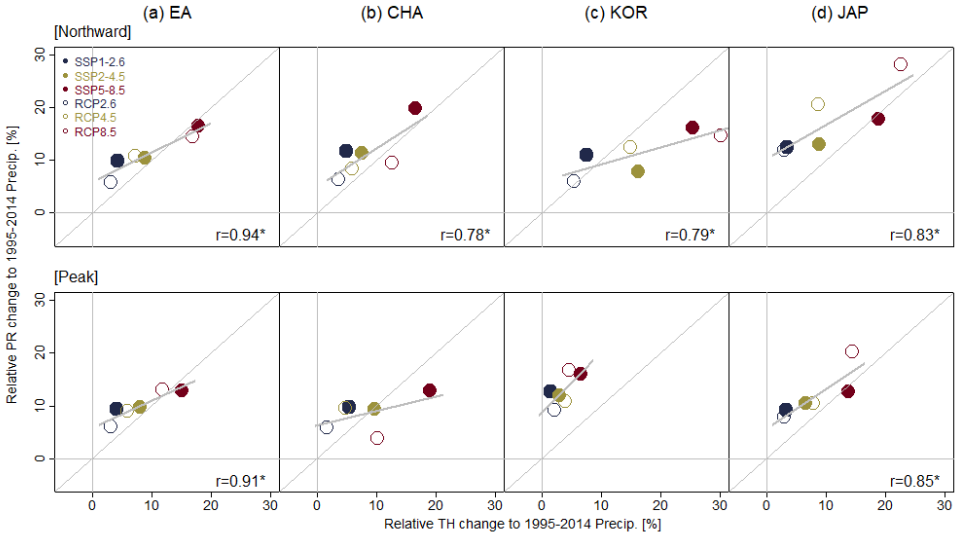

290 **Figure 6. Scatter plot of the mean multi-model ensemble (MME) precipitation change (PR) and thermodynamic (TH) terms, with three climate change scenarios being used in each of the CMIP6 (closed circles) and CMIP5 (open circles) models for long-term (2081–2100) analyses covering (a) East Asia (EA), (b) China (CHA), (c) Korea (KOR), and (d) Japan (JAP). Projection were calculated relative to the climatology precipitation data from 1995–2014. Gray lines represent the linear regression slopes (with statistical significance at the 10% level). Different circle formats represent results obtained using the following climate change**
295 **scenarios: Shared Socioeconomic Pathway (SSP)1-2.6 (closed blue circle), SSP2-4.5 (closed green circle), SSP5-8.5 (closed red circle), Representative Concentration Pathway (RCP)2.6 (open blue circle), RCP4.5 (open green circle), and RCP8.5 (open red circle).**

https://doi.org/10.5194/esd-2024-34
Preprint. Discussion started: 30 October 2024

Earth System Dynamics
Discussions
Open Access
EGU

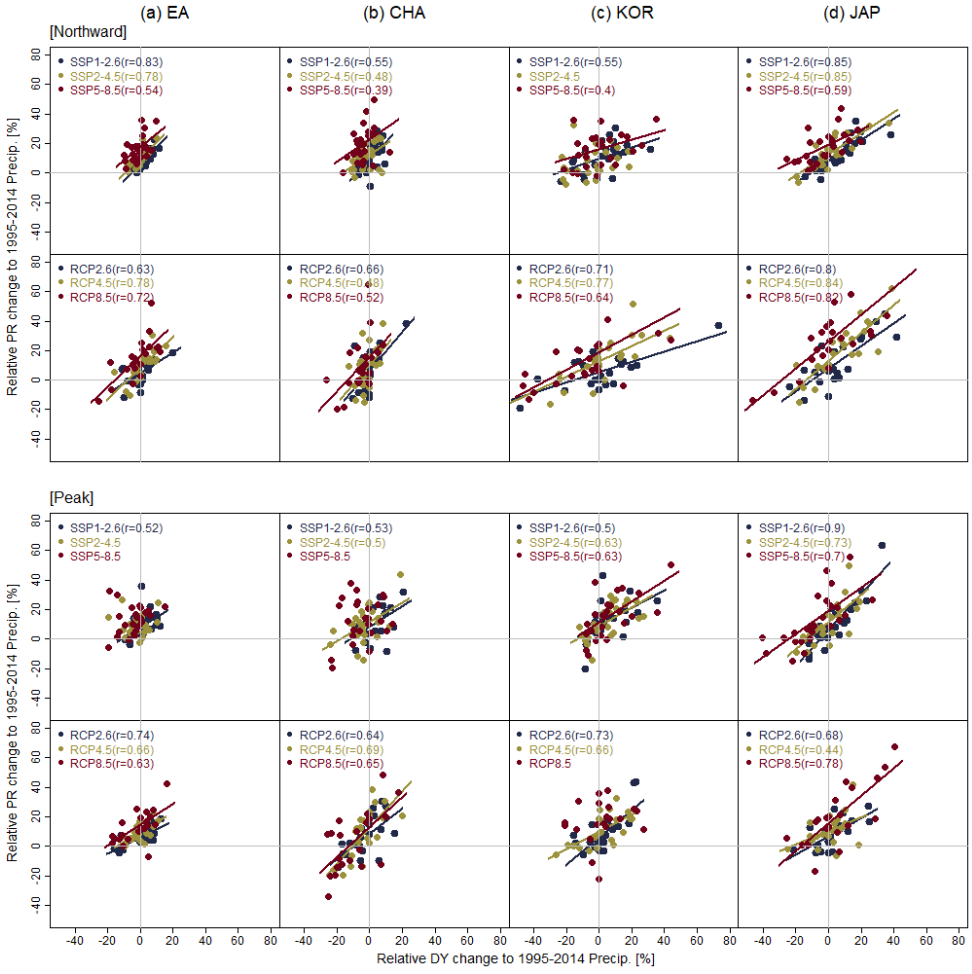

Figure 7. Scatter plot of precipitation change (PR) and dynamic (DY) terms for long-term (2081-2100) analyses covering (a) East Asia (EA), (b) China (CHA), (c) Korea (KOR), and (d) Japan (JAP). Future changes were calculated relative to the from 1995–2014. 300 **Colored lines represent the linear regression slopes (with statistical significance at the 10% level), along with their associated correlation coefficients (r).**

https://doi.org/10.5194/esd-2024-34
Preprint. Discussion started: 30 October 2024

Earth System Dynamics Discussions

Data availability

The utilized CMIP5 and CMIP6 model simulations are listed in table s1 and table s2. All of the datasets can be accessed at https://esgf-node.llnl.gov/search/cmip5/ and https://esgf-node.llnl.gov/search/cmip6/, respectively.

Author contributions

SKM conceived the study; YHK conducted the analysis and wrote the manuscript draft; SKM reviewed and edited the manuscript.

Competing interests

The authors declare that they have no conflict of interest.

Acknowledgements

This study was supported by the Korea Meteorological Administration Research and Development Program under Grant KMI2022-01313 and the Human Resource Program for Sustainable Environment in the 4th Industrial Revolution Society

References

Adler, R. F., Sapiano, M. R. P., Huffman, G. J., Wang, J.-J., Gu, G., Bolvin, D., Chiu, L., Schneider, U., Becker, A., Nelkin, E., Xie, P., Ferraro, R., and Shin, D.-B.: The Global Precipitation Climatology Project (GPCP) Monthly Analysis (New Version 2.3) and a Review of 2017 Global Precipitation, Atmosphere, 9, 138, https://doi.org/10.3390/atmos9040138, 2018.

Chen, Z., Zhou, T., Zhang, L., Chen, X., Zhang, W., and Jiang, J.: Global land monsoon precipitation changes in CMIP6 projections, Geophy. Res. Let., 47, e2019GL086902, https://doi.org/10.1029/2019GL086902, 2020.

Chen, C.-A., Hsu, H.-H., and Liang, H.-C.: Evaluation and comparison of CMIP6 and CMIP5 model performance in simulating the seasonal extreme precipitation in the Western North Pacific and East Asia, Weather Clim. Extremes, 31, 100303, https://doi.org/10.1016/j.wace.2021.100303, 2021.

Endo, H. and Kitoh, A.: Thermodynamic and dynamic effects on regional monsoon rainfall changes in a warmer climate, Geophy. Res. Let., 41, 1704–1711, https://doi.org/10.1002/2013GL059158, 2014.

https://doi.org/10.5194/esd-2024-34
Preprint. Discussion started: 30 October 2024

Eyring, V., Bony, S., Meehl, G. A., Senior, C. A., Stevens, B., Stouffer, R. J., and Taylor, K. E.: Overview of the Coupled Model Intercomparison Project Phase 6 (CMIP6) experimental design and organization, Geosci. Model Dev., 9, 1937–1958, https://doi.org/10.5194/gmd-9-1937-2016, 2016.

Eyring, V., Cox, P. M., Flato, G. M., Gleckler, P. J., Abramowitz, G., Caldwell, P., Collins, W. D., Gier, B. K., Hall, A. D., Hoffman, F. M., Hurtt, G. C., Jahn, A., Jones, C. D., Klein, S. A., Krasting, J. P., Kwiatkowski, L., Lorenz, R., Maloney, E., Meehl, G. A., Pendergrass, A. G., Pincus, R., Ruane, A. C., Russell, J. L., Sanderson, B. M., and Williamson, M. S.: Taking climate model evaluation to the next level, Nat. Clim. Chang., 9, 102–110, https://doi.org/10.1038/s41558-018-0355-y, 2019.

Freychet, N., Hsu, H. H., Chou, C., and Wu, C. H.: Asian summer monsoon in CMIP5 projections: A link between the change in extreme precipitation and monsoon dynamics, J. Climate, 28, 1477–1493, https://doi.org/10.1175/JCLI-D-14-00449.1, 2015.

Gao, Y, Leung, L. R., Salathé Jr., E. P., Dominguez, F., Nijssen, B., and Lettenmaier, D. P.: Moisture flux convergence in regional and global climate models: Implications for droughts in the southwestern United States under climate change, Geophys. Res. Let., 39, L09711, https://doi.org/10.1029/2012GL051560, 2012.

Haarsma, R. J., Roberts, M. J., Vidale, P. L., Senior, C. A., Bellucci, A., Bao, Q., Chang, P., Corti, S., Fučkar, N. S., Guemas, V., von Hardenberg, J., Hazeleger, W., Kodama, C., Koenigk, T., Leung, L. R., Lu, J., Luo, J.-J., Mao, J., Mizielinski, M. S., Mizuta, R., Nobre, P., Satoh, M., Scoccimarro, E., Semmler, T., Small, J., and von Storch, J.-S.: High Resolution Model Intercomparison Project (HighResMIP v1.0) for CMIP6, Geosci. Model Dev., 9, 4185–4208, https://doi.org/10.5194/gmd-9-4185-2016, 2016.

Ha, K.-J., Moon, S., Timmermann, A., and Kim, D.: Future changes of summer monsoon characteristics and evaporative demand over Asia in CMIP6 simulations, Geophys. Res. Let., 47, e2020GL087492, https://doi.org/10.1029/2020GL087492, 2020.

Hawkins, E. and Sutton, R.: The potential to narrow uncertainty in regional climate predictions, Bull. Am. Meteorol. Soc., 90(8), 1095–1108, https://doi.org/10.1175/2009BAMS2607.1, 2009.

Hawkins, E. and Sutton, R.: The potential to narrow uncertainty in projections of regional precipitation change, Clim. Dyn., 37(1–2), 407–418, https://doi.org/10.1007/s00382-010-0810-6, 2011.

Hoegh-Guldberg, O., Jacob, D., Taylor, M., Bindi, M., Brown, S., Camilloni, I., Diedhiou, A., Djalante, R., Ebi, K. L., Engelbrecht, F., Guiot, J., Hijioka, Y., Mehrotra, S., Payne, A., Seneviratne, S. I., Thomas, A., Warren, R., and Zhou, G.: Impacts of 1.5°C global warming on natural and human systems, in: Global Warming of 1.5°C. An IPCC Special Report on the impacts of global warming of 1.5°C above pre-industrial levels and related global greenhouse gas emission pathways, in the context of strengthening the global response to the threat of climate change, sustainable development, and efforts to eradicate poverty, edited by: Masson-Delmotte, V., Zhai, P., Pörtner, H.-O., Roberts, D., Skea, J., Shukla, P. R., Pirani, A., Moufouma-Okia, W., Péan, C., Pidcock, R., Connors, S., Matthews, J. B. R., Chen, Y., Zhou, X., Gomis, M. I., Lonnoy, E., Maycock, T., Tignor, M., and Waterfield, T., In Press, 2018.

https://doi.org/10.5194/esd-2024-34
Preprint. Discussion started: 30 October 2024

IPCC: Climate Change 2013: The Physical Science Basis. Contribution of Working Group I to the Fifth Assessment Report of the Intergovernmental Panel on Climate Change, edited by: Stocker, T. F., Qin, D., Plattner, G.-K., Tignor, M., Allen, S. K., Boschung, J., Nauels, A., Xia, Y., Bex, V., and Midgley, P. M., Cambridge University Press, Cambridge, United Kingdom and New York, NY, USA, 1535 pp., 2013.

Kim, Y.-H., Min, S.-K., Zhang, X., Sillmann, J., and Sandstad, M.: Evaluation of the CMIP6 multi-model ensemble for climate extreme indices, Weather. Clim. Extremes, 29, 100269, https://doi.org/10.1016/j.wace.2020.100269, 2020.

Kitoh, A., Endo, H., Kumar, K. K., Cavalcanti, I. F. A., Goswami, P., and Zhou, T.: Monsoons in a changing world: a regional perspective in a global context, J. Geophys. Res. Atmos., 118, 3053–3065, https://doi.org/10.1002/jgrd.50258, 2013.

Kusunoki, S. and Arakawa, O.: Are CMIP5 models better than CMIP3 models in simulating precipitation over East Asia? J. Climate, 28(14), 5601–5621, https://doi.org/10.1175/JCLI-D-14-00585.1, 2015.

Lee, D., Min, S.-K., Jin, J., Lee, J.-W., Cha, D.-H., Suh, M.-S., Ahn, J.-B., Hong, S.-Y., Kang, H.-S., and Joh, M.: Thermodynamic and dynamic contributions to future changes in summer precipitation over Northeast Asia and Korea: A multi-RCM study, Clim. Dyn., 49(11), 4121-4139, https://doi.org/10.1007/s00382-017-3566-4, 2017.

Lee, D., Min, S.-K., Fischer, E., Shiogama, H., Bethke, I., Lierhammer, L., and Scinocca, J.: Impacts of half a degree additional warming on the Asian summer monsoon rainfall characteristics, Environ. Res. Let., 13, https://doi.org/10.1088/1748-9326/aab55d, 044033, 2018.

Lehner, F., Deser, C., Maher, N., Marotzke, J., Fischer, E. M., Brunner, L., Knutti, R., and Hawkins, E.: Partitioning climate projection uncertainty with multiple large ensembles and CMIP5/6, Earth Syst. Dynam., 11, 491–508, https://doi.org/10.5194/esd-11-491-2020, 2020.

Marotzke, J., Jakob, C., Bony, S., Dirmeyer, P. A., O'Gorman, P. A., Hawkins, E., Perkins-Kirkpatrick, S., Le Quéré, C., Nowicki, S., Paulavets, K., Seneviratne, S. I., Stevens, B., and Tuma, M.: Climate research must sharpen its view, Nat. Clim. Chang., 7, 89–91, https://doi.org/10.1038/nclimate3206, 2017.

Moon, S. and Ha, K.-J.: Future changes in monsoon duration and precipitation using CMIP6, npj Clim. Atmos. Sci., 3, 45, https://doi.org/10.1038/s41612-020-00151-w, 2020,

Jiang, C., Hu, D., Tian, Z., and Lang, Z.: Differences between CMIP6 and CMIP6 models in simulating climate over China and the East Asian monsoon, Adv. Atmos. Sci., 37, 1102-1118, https://doi.org/10.1007/s00376-020-2034-y, 2020.

Li, X., Ting, M., Li, C., and Henderson, N.: Mechanisms of Asian summer monsoon changes in response to anthropogenic forcing in CMIP5 models, J. Climate, 28, 4107–4125, https://doi.org/10.1175/JCLI-D-14-00559.1, 2015.

O'Neill, B. C., Tebaldi, C., van Vuuren, D. P., Eyring, V., Friedlingstein, P., Hurtt, G., Knutti, R., Kriegler, E., Lamarque, J.-F., Lowe, J., Meehl, G. A., Moss, R., Riahi, K., and Sanderson, B. M.: The Scenario Model Intercomparison Project (ScenarioMIP) for CMIP6, Geosci. Model Dev., 9, 3461–3482, https://doi.org/10.5194/gmd-9-3461-2016, 2016.

Paik, S., Min, S.-K., Zhang, X., Donat, M. G., King, A. D., and Sun, Q.: Determining the anthropogenic greenhouse gas contribution to the observed intensification of extreme precipitation, Geophys. Res. Let., 47, e2019GL086875, https://doi.org/10.1029/2019GL086875, 2020.

https://doi.org/10.5194/esd-2024-34
Preprint. Discussion started: 30 October 2024

Park, C. and Min, S.-K.: Multi-RCM near-term projections of summer climate extremes over East Asia, Clim. Dynam., 52, 4937–4952, https://doi.org/10.1007/s00382-018-4425-7, 2019.

Seager, R. and Naik, N.: A mechanisms-based approach to detecting recent anthropogenic hydro climate change, J. Climate, 25 236–261, https://doi.org/10.1175/JCLI-D-11-00056.1, 2012.

Taylor, K. E., Stouffer, R. J. and Meehl, G. A.: An overview of CMIP5 and the experiment design, Bull. Am. Meteorol. Soc. 93, 485-498, https://doi.org/10.1175/BAMS-D-11-00094.1, 2012.

Wang, B., Biasutti, M., Byrne, M. P., Castro, C., Chang, C.-P., Cook, K., Fu, R., Grimm, A. M., Ha, K.-J., Hendon, H., Kitoh, A., Krishnan, R., Lee, J.-Y., Li, J., Liu, J., Moise, A., Pascale, S., Roxy, M. K., Seth, A., Sui, C.-H., Turner, A., Yang, S., Yun, K.-S., Zhang, L., and Zhou, T.: Monsoons climate change assessment, Bull. Am. Meteorol. Soc., 102, E1–E19, https://doi.org/10.1175/BAMS-D-19-0335.1, 2021.

Wehner, M., Lee, J., Risser, M., Ullrich, P., Gleckler, P., and Collins, W. D.: Evaluation of extreme sub-daily precipitation in high-resolution global climate model simulations, Phil. Trans. R. Soc. A, 379, 20190545, https://doi.org/10.1098/rsta.2019.0545, 2021.

Xie, P. and Arkin, P.: Global precipitation: A 17-year monthly analysis based on gauge observations, satellite estimates, and numerical model outputs, Bull. Am. Meteorol. Soc., 78, 2539–2558, https://doi.org/10.1175/1520-0477(1997)078<2539:GPAYMA>2.0.CO;2, 1997.

Xin, X., Wu, T., Zhang, J., Yao, J., and Fang, Y.: Comparison of CMIP6 and CMIP5 simulations of precipitation in China and the East Asian summer monsoon, Int. J. Climatol., 40, 6423-6440, https://doi.org/10.1002/joc.6590, 2020.

Xin, X., Wu, T., Jie, W., and Zhang. J.: Impact of Higher Resolution on Precipitation over China in CMIP6 HighResMIP Models, Atmosphere, 12, 762, https://doi.org/10.3390/atmos12060762, 2021.

Zhou, T., Lu, J., Zhang, W., and Chen, Z.: The sources of uncertainty in the projection of global land monsoon precipitation, Geophys. Res. Let., 47, e2020GL088415, https://doi.org/10.1029/2020GL088415, 2020.